01 Oct 2007

Triple-Differential Cross Sections for Target Ionization with Simultaneous Projectile Detachment in 200-keV H^- + He Collisions

T. Ferger

Michael Schulz
Missouri University of Science and Technology, schulz@mst.edu

Daniel Fischer
Missouri University of Science and Technology, fischerda@mst.edu

B. Najjari

et. al. For a complete list of authors, see https://scholarsmine.mst.edu/phys_facwork/412

Recommended Citation

T. Ferger et al., "Triple-Differential Cross Sections for Target Ionization with Simultaneous Projectile Detachment in 200-keV H^- + He Collisions," *Physical Review A: Atomic, Molecular, and Optical Physics*, vol. 76, no. 4, pp. 042708-1-042708-6, American Physical Society (APS), Oct 2007.
The definitive version is available at https://doi.org/10.1103/PhysRevA.76.042708

Triple-differential cross sections for target ionization with simultaneous projectile detachment in 200-keV H^-+He collisions

T. Ferger,[1] M. Schulz,[2] D. Fischer,[3] B. Najjari,[1] R. Moshammer,[1] and J. Ullrich[1]
[1]*Max-Planck-Institut für Kernphysik, Saupfercheckweg 1, 69117 Heidelberg, Germany*
[2]*University of Missouri-Rolla, Physics Department and LAMOR, Rolla, Missouri 65409, USA*
[3]*Stockholm University, Atomic Physics, Alba Nova, S-106 91 Stockholm, Sweden*
(Received 18 July 2007; published 10 October 2007)

We have performed a kinematically complete experiment for target ionization with simultaneous projectile detachment (TIPD) in 200-keV H^-+He collisions. From the data we extracted triple-differential cross sections (TDCSs) for each electron separately. These TDCSs closely resemble corresponding data for single ionization by charged-particle impact. Surprisingly, the contributions from higher-order processes to TIPD, proceeding through two independent interactions of each electron with the core of the respective other collision partner, are found to be somewhat larger than the first-order process proceeding through the electron-electron interaction.

DOI: 10.1103/PhysRevA.76.042708 PACS number(s): 34.50.Fa, 34.10.+x

I. INTRODUCTION

Studies of fragmentation processes in simple atomic collision systems have provided rich information about the fundamentally important few-body problem [1,2]. Especially single ionization of light atoms by charged particle impact has been studied in great detail (e.g., [3–5]). Experimental data of fully differential cross sections (FDCSs) have proven to provide very sensitive tests of theoretical models (e.g., [1,6–11]). For processes involving multiple-electron transitions, in contrast, the literature is not nearly as comprehensive. In the case of double ionization of helium, for example, FDCSs are only available for electron impact [12,13] and only one data set of nearly fully differential cross sections for ion impact has been reported [14].

One aspect of the dynamical few-body problem in collisions which is particularly relevant in multiple-electron transitions is the role of the electron-electron interaction. Although it can be very important in, e.g., double ionization (in contrast to single ionization), it cannot cause the electronic transition alone, but rather it is always accompanied by an interaction of the projectile with at least one electron. In this regard, another process involving a two-electron transition—simultaneous electron ejection from both collision partners—is fundamentally different from double ionization: here, the process can proceed through a single electron-electron interaction while the cores of the collision partners remain essentially passive. Indeed, such a first-order mechanism has been identified in mutual ionization in F^{8+}+He [15] and He^++He [16] collisions.

As for double ionization, measured multiple-differential cross sections for simultaneous electron ejection from both collision partners are rare. Probably the most detailed data currently available are those of Kollmus *et al.* [17] for 3.6 MeV/amu C^{2+}+He. There, the cross sections were presented in a similar way as in a typical fully differential study of electron impact ionization $(e,2e)$: for projectile electrons ejected into the scattering plane, defined by the initial and final target-atom momenta, the cross sections were plotted as a function of the polar-electron ejection angle and the momentum transfer q (difference between the initial and final target atom momenta). However, the data were integrated over the energy of the projectile electron and over all kinematic quantities of the target electron. Nevertheless, the characteristic features in the electron angular distribution, familiar from the FDCSs for pure target ionization, with a binary peak approximately in the direction of q and a recoil peak approximately in the direction of $-q$, were observed.

More recently, multiple-differential cross sections for simultaneous target ionization and projectile detachment (TIPD) were reported for 200-keV H^-+He collisions [18–20]. An important difference from the collision systems studied in Refs. [15–17] is that the active projectile electron is initially very weakly bound (0.7 eV). It therefore seems reasonable to view the incoming H^- projectile as a H^0 atom and a separate, quasifree electron. In such a situation one might expect that it is easier to separate the first-order process, proceeding through a single electron-electron interaction, from higher-order processes, proceeding through two independent interactions between each electron and the respective other collision partner, than in cases where both electrons are initially relatively tightly bound. Instead, the reaction dynamics proved surprisingly complex. Only after a novel data analysis technique had been developed, in which multiple-differential cross sections are plotted as a function of all four collision fragments simultaneously in a single spectrum using a tetrahedral coordinate system, could signatures of the first-order process be unambiguously identified [20].

The new data analysis technique introduced in Ref. [20] is very powerful in extracting a qualitative, comprehensive picture of the reaction dynamics from the measured data. However, calculations of the corresponding cross sections are not straightforward. To test theoretical models sensitively on a quantitative level measured FDCSs are more feasible. A comparison of such data with theory can also provide more detailed information about the relative importance of first- and higher-order contributions to the cross sections. Unfortunately, the total number of TIPD events collected in this experiment is not sufficient to extract statistically meaningful FDCSs. However, in this article we do present FDCSs integrated over the kinematic parameters of one of the ejected

electrons. Such data correspond to cross sections differential in the energy and solid angle of one electron and in the scattered projectile solid angle—i.e., to triple-differential cross sections TDCS. Depending on whether the FDCSs are integrated over the target or projectile electron, we refer to these cross sections as projectile or target TDCSs. The data are presented in the same form as those of Kollmus *et al.* [17], but are more detailed in that they are not integrated over both electron energies.

II. EXPERIMENT

The experiment was performed at the Max-Planck-Institut für Kernphysik in Heidelberg. A H^- beam was generated with a Duoplasmatron ion source and accelerated to 200 keV. The projectile beam was crossed with a very cold ($T \approx 1.5$ K) neutral He beam from a supersonic gas jet with a density of about 10^{11} atoms/cm^2. The projectiles which were neutralized in the collision (and which were selected by deflecting the charged beam components out using a magnet) were detected by a channel plate detector. The recoil ions and the ionized electrons were extracted in the longitudinal direction (defined by the initial projectile direction) by a weak electric field of 2.3 V/cm. A uniform magnetic field of 15 G confined the transverse motion of the electrons so that all electrons with a transverse momentum of less than 2.5 a.u. were guided onto the detector.

The momentum vectors of the recoil ions and the ejected electrons as well as the recoil ion charge state were determined by using position-sensitive detectors and time-of-flight techniques, where a fast signal from the projectile detector served as a timing reference. The momentum resolutions depend on the momenta themselves, and therefore averaged values are provided. In the longitudinal direction, defined by the projectile beam axis (z direction), they are 0.15 a.u. and 0.01 a.u. for the recoil ion and for the electrons, respectively [in all cases the full width at half maximum (FWHM) is provided]. In the transverse direction the corresponding numbers are 0.35 a.u. and 0.1 a.u. (for a more detailed discussion of the resolution see Refs. [21,22]).

For each event both electrons were detected simultaneously with a single detector employing a multihit technique (dead time ≈ 10 ns). It should be noted that since one electron is emitted from the moving projectile frame and one from the target frame at rest, their time of flight is in most cases very different. As a result, losses due to the multihit dead time are not as critical as in double-ionization experiments using this method. The momentum of the neutralized projectiles was determined from momentum conservation. From the electron momenta it is straightforward to calculate the emission angles.

III. RESULTS AND DISCUSSION

In the following we will discuss the target- and projectile-electron spectra separately. The latter will be analyzed in the rest frame of the incoming H^- ion, and in this "reversed" kinematics we view the helium atom as the projectile. For clarity, we will therefore use the terms H^- projectile when we refer to target-electron ejection and He projectile when we refer to projectile-electron ejection. Note, however, that the magnitude of the momentum transfer q is identical in both cases. We restrict the discussion to electrons ejected into the scattering plane. As mentioned above, the data for the ejection of each electron are integrated over all coordinates of the respective other electron.

A. Target-electron ejection

In Fig. 1 the TDCSs for ejection of target electrons with an energy of 10 ± 2 eV are plotted for transverse momentum transfers q_t of 0.9 ± 0.1 a.u. (top), 1.3 ± 0.1 a.u. (center), and 1.5 ± 0.1 a.u. (bottom). Electrons ejected into the scattering plane within $\pm 10°$ are accepted. The characteristic double-lobe structure familiar from $(e,2e)$ studies with a binary peak between 60° and 90° and a recoil peak between 180° and 210° is clearly visible. The data are not absolutely normalized, but they are normalized correctly relative to each other.

As mentioned above, it seems reasonable to treat the incoming H^- projectile as a H^0 atom and a separate, quasifree electron because of the very small binding energy. One may further suspect that the neutral H^0 core does not significantly contribute to target-electron ejection. Under these assumptions we would then expect the target TDCS to resemble those for ionization by free electron impact under the same kinematic conditions. Such data were recently published by Dürr *et al.* for 102 eV e^-+He [23], which corresponds to almost the same projectile velocity as 200 keV H^-. These data, which were scaled to match the peak heights in the target TDCS for H^- impact, are shown in Fig. 1 for $E_e = 10$ eV and $q_t = 0.9$ a.u. as open symbols. For the other momentum transfers free-electron-impact data are not available.

The angular dependences of the TDCS for free electron and H^- impact agree very well. Only in the minimum separating the binary and recoil peaks from each other are some differences observed. The data for H^- impact are thus not inconsistent with the notion that target-electron ejection is largely caused by the loosely bound electron on the initial H^- projectile. However, it would be premature to conclude that target ionization by the H^0 core does not play a significant role. Both the electron and proton on the projectile core may cause target-electron ejection, although to an observer at large distance their electric charges neutralize each other. The electron remaining bound to the projectile is in the initial state indistinguishable from the ejected projectile electron. Therefore, it is not unreasonable to expect that target ionization by both electrons leads to the same angular dependence of the TDCS. For proton impact the first Born approximation (FBA) predicts identical TDCSs as for electron impact, as well. On the other hand, higher-order contributions generally do depend on the charge sign of the projectile, where for negatively charged particles the peak structures are usually shifted in the backward direction relative to the FBA and for positively charged particles in the forward direction. However, such effects may not be strong enough to be visible in the measured cross sections, especially if the contributions from proton impact are not large.

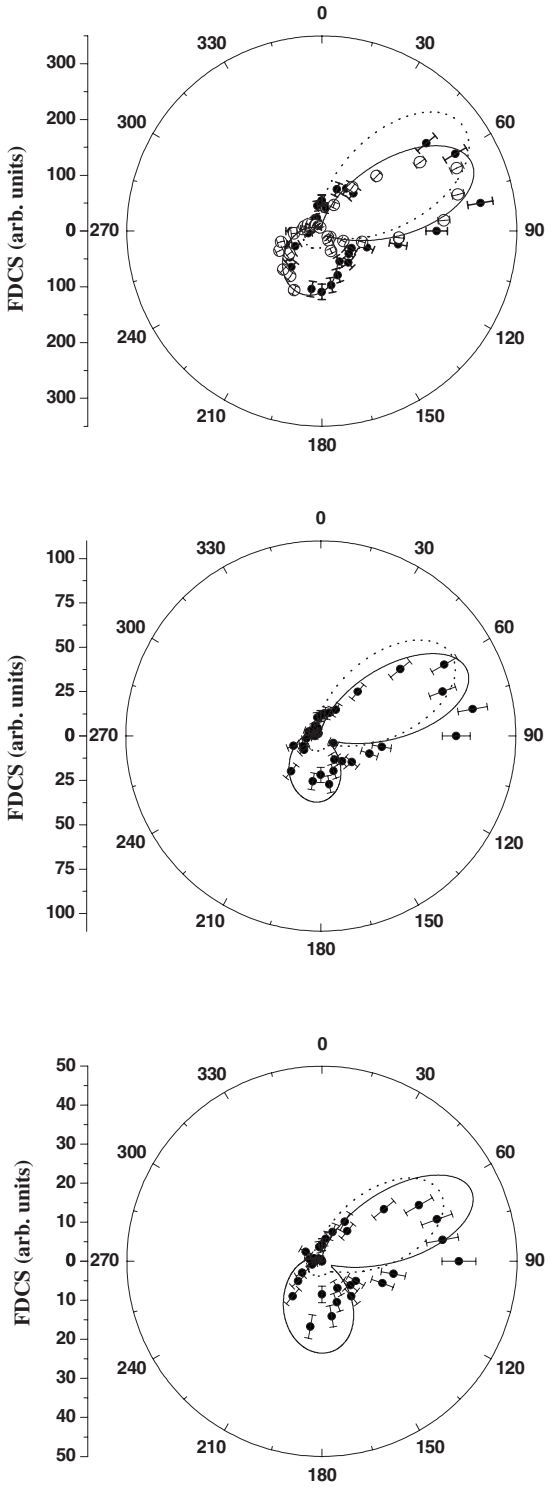

FIG. 1. Triple-differential cross sections for simultaneous electron ejection from the projectile and the target in 200-keV H^- +He collisions (solid symbols). The data are integrated over all projectile electron parameters and shown for target electrons with an energy of 10 eV ejected into the scattering plane. The transverse momentum transfer is fixed at 0.9 a.u. (top), 1.3 a.u. (center), and 1.5 a.u. (bottom). The open symbols represent data for single target ionization in 102-eV e^-+He collisions [23]. Dotted curve: first Born approximation. Solid curve: 3C approximation for target ionization by free electron impact.

The FBA, shown as dotted curves in Fig. 1, only contains the first-order process in which the ejection of both electrons proceeds through the electron-electron interaction. The H^- projectile is described in terms of a Yukawa potential [18]. Not surprisingly, it is in poor agreement with the data. The position of the binary peak, which in the FBA coincides with the direction of q, is shifted in the forward direction relative to the data for all q and the intensity of the recoil peak is drastically underestimated. The solid curves show calculations based on the three-body Coulomb wave function (3C) approximation [24] for single target ionization by free electron impact; i.e., here simultaneous ejection of both electrons by two independent interactions of each electron with the respective other collision partner is not accounted for either. However, higher-order contributions in the projectile electron-target atom interaction, generally dubbed post-collision interaction (PCI), are included. For $q=0.9$ a.u. the agreement with the data for both H^- and free electron impact is quite nice; however, with increasing q increasing deviations are observed. These discrepancies may be due to the limitations of the 3C model becoming more important at larger q. However, it is also conceivable that with increasing q target electron ejection by the H^0 core becomes increasingly important or that it leads to increasing differences in the angular dependence of the target TDCS compared to free electron impact. More information about the relative importance of the processes proceeding through a single electron-electron interaction or two independent interactions of each electron with the respective other collision partner is contained in the TDCS for projectile-electron ejection.

B. Projectile-electron ejection

In the top panel of Fig. 2 the projectile TDCSs are plotted in the rest frame of the H^- projectile for an ejected electron energy of 10 ± 2 eV and a momentum transfer of 0.9 ± 0.1 a.u. The 0° angle (or the forward direction) is defined by the direction of the incoming He projectile. While a pronounced binary peak at about 40° is found, the recoil peak is, in contrast to target-electron ejection, completely absent. The solid curve shows the FBA using a Yukawa potential for the H^- projectile. A higher-order calculation for simultaneous ejection of both electrons with a Yukawa potential is currently not feasible. Large discrepancies between the FBA and the data are quite obvious. The backward shift in the binary peak position relative to the data is expected and will be discussed below. First, we will analyze the width of the measured angular distribution, which is drastically underestimated by the FBA.

In contrast to the FBA the measured projectile TDCSs are not symmetric about the centroid of the peak. Instead, a "shoulder" can be seen superimposed on the small-angle wing of the binary peak. This shape suggests that the binary peak may contain two contributions, possibly one originating from target-electron impact and one from He^+ impact. To test this hypothesis we attempted to separate these contributions by setting conditions on the ratio between the recoil-ion momentum p_{rec} and the target-electron momentum p_{elt}. If the projectile-electron ejection was caused by the target electron

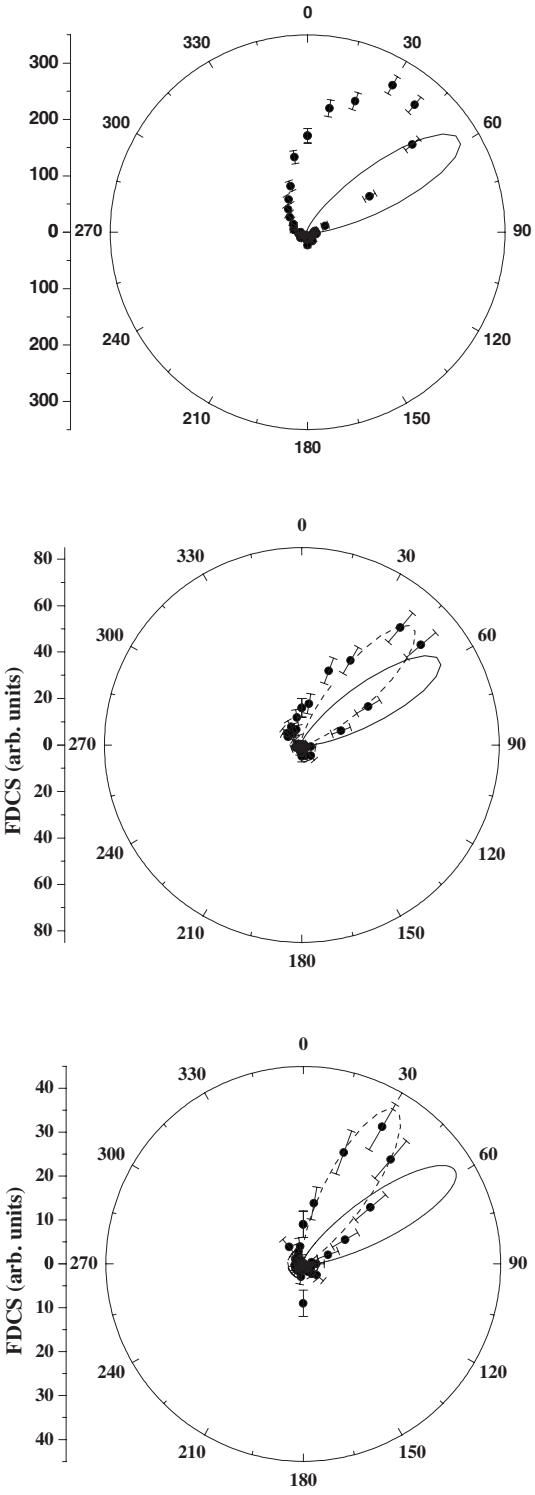

FIG. 2. Triple-differential cross sections for simultaneous electron ejection from the projectile and the target in 200-keV H^- +He collisions (top). The data are integrated over all target electron parameters and shown in the rest frame of the initial H^- projectile for projectile electrons with an energy of 10 eV ejected into the scattering plane. The transverse momentum transfer is fixed at 0.9 a.u. For the plots in the center and the bottom the additional conditions $p_{rec} > 3p_{elt}$ and $p_{elt} > 3p_{rec}$, respectively, were set. Solid curve: first Born approximation. Dashed curve: first Born approximation shifted to match the peak position in the data.

and the He^+ ion remained essentially passive, then p_{elt} should be larger than p_{rec} and vice versa. We therefore generated the projectile TDCSs with the additional condition $p_{rec} > 3p_{elt}$ (center of Fig. 2) and $p_{elt} > 3p_{rec}$ (bottom of Fig. 2) and associate them with projectile-electron ejection by He^+ and target-electron impact, respectively. Indeed, both conditions lead to a significantly narrower binary peak. We also note that in the electron-impact case the binary peak is pointing more in the forward direction than in the He^+-impact case. To compare the widths in the data and in the FBA we shifted the theoretical TDCSs so that the peak position coincides with those in the data (dashed curves). Now the measured and calculated widths are in good agreement, suggesting that the association of the spectra for the conditions $p_{rec} > 3p_{elt}$ and $p_{elt} > 3p_{rec}$ with projectile-electron ejection by He^+ and target-electron impact, respectively, is correct.

The reason for the forward shift of the binary peak in the experimental data relative to the FBA is different for He^+ impact than for electron impact. In the FBA for single target ionization (i.e., without projectile-electron ejection) the binary peak is necessarily centered on the direction of q. In the present case of projectile-electron ejection accompanied by target ionization there are three factors which could potentially lead to a significant shift of the binary peak: (i) PCI usually leads to a forward shift for positively charged ion impact and to a backward shift for electron impact [5]. (ii) Elastic scattering between the cores of the collision partners can lead to a backward shift at very small q and to a forward shift at larger q, independent of the sign of the projectile charge [9,10]. (iii) If the projectile-electron ejection is caused by the target electron in the first-order process, then the target-electron ejection is likely to be caused by the projectile electron. Therefore, in the rest frame of the initial helium atom the projectile electron loses an energy which is at least as large as the ionization potential of helium. In the rest frame of the H^- ion this energy loss corresponds to a longitudinal momentum in the direction of the incoming target atom—i.e., in the forward direction. This momentum is added to the longitudinal momentum transferred to the projectile electron by the target atom. Consequently, the projectile electron momentum is shifted in the forward direction relative to q in the rest frame of the initial H^- projectile.

The peak positions in the spectra of Fig. 2 can now be explained as follows: in the case of He^+ impact, the binary peak is shifted forward by PCI and possibly by elastic scattering. For electron impact, PCI alone would shift the binary peak backward; however, it is outweighed by a much larger forward shift due to the energy loss resulting from the target ionization (and, as in the He^+-impact case, possibly by elastic scattering). The latter effect is even strong enough to make the forward shift for electron impact larger than for He^+ impact. The longitudinal projectile-electron momentum due to the energy loss caused by the target ionization is at least 0.32 a.u. and increases with increasing target-electron energy. This corresponds to a minimum forward shift of about 20°. The backward shift due to PCI cannot be estimated easily. However, the free-electron-impact ionization data for helium provide an upper limit of about 10° for the kinematic condition considered here (see top panel of Fig. 1). For electron ejection from H^- PCI is expected to be much weaker

because of the much smaller binding energy and the smaller effective charge of the core. The effect of elastic scattering is even more difficult to evaluate. It is not even clear whether at this particular q of 0.9 a.u. it causes a forward or a backward shift (although based on the data reported in Refs. [9,10] a forward shift seems more likely). Nevertheless, this analysis qualitatively supports the notion that the forward shift in the electron-impact case, and the observation that this shift is more pronounced than in the He^+-impact case, is mainly due to the energy loss caused by target ionization.

The intensities of the spectra of Fig. 2 provide a crude estimate of the relative importance of the first-order process (proceeding through the electron-electron interaction) and the higher-order process (proceeding through two independent interactions between each electron and the respective other collision partner). The conditions set for the lower two spectra do not constitute an exact selection of these contributions, and using a factor of 3 for the momentum ratio in the conditions is somewhat arbitrary. Nevertheless, as a qualitative estimate one can state that the first-order process is somewhat weaker than the independent process; the intensities of the corresponding spectra in Fig. 2 suggest a ratio of roughly 1:2. This estimate, which also holds for target-electron ejection, is consistent with an analysis based on four-particle Dalitz plots which we recently presented [20].

IV. CONCLUSIONS

We have presented triple-differential cross sections for simultaneous target ionization and projectile detachment in 200-keV H^-+He collisions. The presentation of the data is equivalent to common presentations of fully differential cross sections for single ionization by free electron impact. We could therefore directly compare our TDCSs for target-electron ejection to data measured for 102-eV e^-+He collisions [23], which corresponds to nearly the same projectile velocity as the collision system studied here. The two data sets exhibit essentially the same angular distribution of the TDCSs. Nevertheless, this similarity does not imply that target-electron ejection is primarily caused by an interaction with the ejected projectile electron.

In the case of projectile-electron ejection two contributions to the TDCSs can crudely be separated, one resulting from target-electron impact and one from He^+ impact. The shape of the angular distributions of the TDCS for both components is well described by the first Born approximation where the H^- projectile is described by a Yukawa potential. However, the data are significantly shifted in the forward direction relative to the FBA. Only for He^+ impact can this shift be attributed to the post-collision interaction between the outgoing He^+ ion and the ejected electron. In the case of electron impact it is due to the energy loss resulting from releasing the target electron from the helium atom. The relative intensities of the TDCSs for He^+ and target-electron impact suggest that the first-order process, proceeding through a single electron-electron interaction, contributes less to TIPD than the higher-order process, proceeding through two independent interactions of each electron with the respective other collision partner.

ACKNOWLEDGMENTS

This work was supported by the Deutsche Forschungsgemeinschaft and the National Science Foundation under Grant No. PHY-0353532.

[1] M. Schulz, R. Moshammer, D. Fischer, H. Kollmus, D. H. Madison, S. Jones, and J. Ullrich, Nature (London) **422**, 48 (2003).
[2] T. N. Rescigno, M. Baertschy, W. A. Isaacs, and C. W. McCurdy, Science **286**, 2474 (1999).
[3] M. E. Rudd, Y.-K. Kim, D. H. Madison, and T. J. Gay, Rev. Mod. Phys. **64**, 441 (1992), and references therein.
[4] H. Ehrhardt, K. Jung, G. Knoth, and P. Schlemmer, Z. Phys. D: At., Mol. Clusters, **1**, 3 (1986), and references therein.
[5] M. Schulz and D. H. Madison, Int. J. Mod. Phys. A **21**, 3649 (2006), and references therein.
[6] J. Röder, H. Ehrhardt, I. Bray, D. V. Fursa, and I. E. McCarthy, J. Phys. B **29**, 2103 (1996).
[7] M. Dürr, C. Dimopoulou, A. Dorn, B. Najjari, I. Bray, D. V. Fursa, Zhangjin Chen, D. H. Madison, K. Bartschat, and J. Ullrich, J. Phys. B **39**, 4097 (2006).
[8] M. Schulz, R. Moshammer, A. N. Perumal, and J. Ullrich, J. Phys. B **35**, L161 (2002).
[9] N. V. Maydanyuk, A. Hasan, M. Foster, B. Tooke, E. Nanni, D. H. Madison, and M. Schulz, Phys. Rev. Lett. **94**, 243201 (2005).
[10] M. Schulz, A. Hasan, N. V. Maydanyuk, M. Foster, B. Tooke, and D. H. Madison, Phys. Rev. A **73**, 062704 (2006).
[11] M. Schulz, R. Moshammer, A. Voitkiv, B. Najjari, and J. Ullrich, Nucl. Instrum. Methods Phys. Res. B **235**, 296 (2005).
[12] A. Dorn, A. Kheifets, C. D. Schröter, B. Najjari, C. Höhr, R. Moshammer, and J. Ullrich, Phys. Rev. Lett. **86**, 3755 (2001).
[13] A. Dorn, A. Kheifets, C. D. Schröter, B. Najjari, C. Höhr, R. Moshammer, and J. Ullrich, Phys. Rev. A **65**, 032709 (2002).
[14] D. Fischer, R. Moshammer, A. Dorn, J. R. Crespo Lopez-Urrutia, B. Feuerstein, C. Höhr, C. D. Schröter, S. Hagmann, H. Kollmus, R. Mann, B. Bapat, and J. Ullrich, Phys. Rev. Lett. **90**, 243201 (2003).
[15] W. Wu, K. L. Wong, R. Ali, C. Y. Chen, C. L. Cocke, V. Frohne, J. P. Giese, M. Raphaelian, B. Walch, R. Dörner, V. Mergel, H. Schmidt-Böcking, and W. E. Meyerhof, Phys. Rev. Lett. **72**, 3170 (1994).
[16] R. Dörner, V. Mergel, R. Ali, U. Buck, C. L. Cocke, K. Froschauer, O. Jagutzki, S. Lencinas, W. E. Meyerhof, S. Nüttgens, R. E. Olson, H. Schmidt-Böcking, L. Spielberger, K. Tökesi, J. Ullrich, M. Unverzagt, and W. Wu, Phys. Rev. Lett. **72**, 3166 (1994).
[17] H. Kollmus, R. Moshammer, R. E. Olson, S. Hagmann, M. Schulz, and J. Ullrich, Phys. Rev. Lett. **88**, 103202 (2002).

[18] T. Ferger, D. Fischer, M. Schulz, R. Moshammer, A. B. Voitkiv, B. Najjari, and J. Ullrich, Phys. Rev. A **72**, 062709 (2005).
[19] M. Schulz, T. Ferger, D. Fischer, R. Moshammer, and J. Ullrich, Phys. Rev. A **74**, 042705 (2006).
[20] M. Schulz, D. Fischer, T. Ferger, R. Moshammer, and J. Ullrich, J. Phys. B **40**, 3091 (2007).
[21] M. Dürr, B. Najjari, M. Schulz, A. Dorn, R. Moshammer, A. B. Voitkiv, and J. Ullrich, Phys. Rev. A **75**, 062708 (2007).
[22] M. Schulz, M. Dürr, B. Najjari, R. Moshammer, and J. Ullrich, Phys. Rev. A **76**, 032712 (2007).
[23] M. Dürr, C. Dimopoulou, A. Dorn, B. Najjari, I. Bray, D. V. Fursa, Zhangjin Chen, D. H. Madison, K. Bartschat, and J. Ullrich, J. Phys. B **39**, 4097 (2006).
[24] M. Brauner, J. S. Briggs, and H. Klar, J. Phys. B **22**, 2265 (1989).